ROUTINE COMPREHENSIVE TISSUE IMAGING ON THE XEVO G3 QTOF MASS SPECTROMETER USING DESI XS

Authors Lisa Reid, Mark Towers, Joanne Ballantyne

Affiliations Waters Corporation, Wilmslow UK

INTRODUCTION

In this poster we investigate the use of the Xevo G3 QTof mass spectrometer coupled with the DESI XS source, which includes the Waters high performance sprayer and heated transfer line, to rapidly acquire a whole murine brain image.

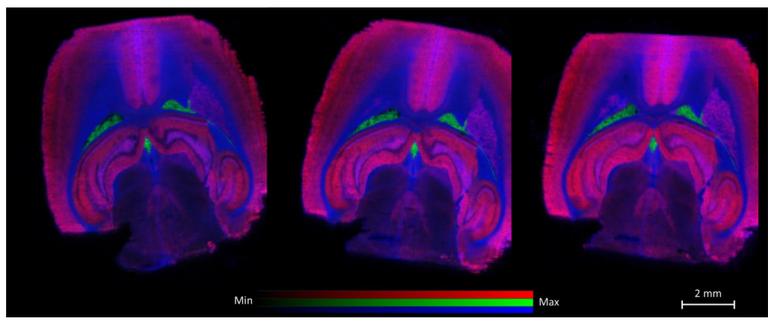

Figure 1: example images, overlay of lipids putatively identified as PS(40:6) red, PS(38:4) green and PE(38:4) blue. 5 scans/second left, 10scans/second middle and 20 scans/second right.

With mass spectrometry tissue imaging experiments, a limiting factor can be the time required for a full tissue image to be created. It has often been observed that the lower the scan rate for which an image is acquired, the intensity of the data achieved is higher and therefore historically the data richer.

We demonstrate that although increasing the data acquisition speed results in a reduction of peak intensity this has little effect on data quality in terms of the relative abundances of lipids, number of detected features and overall analyte distribution.

The Waters™ Xevo™ G3 QTof mass spectrometer provides a powerful, robust and flexible platform for MS imaging analyses. It offers great sensitivity, a dynamic range of up to 5 orders of magnitude, a ~30,000 FWHM mass resolution, and a high mass accuracy.

Being a QTof mass spectrometer mass spectrometer, it has the option of multiple data acquisition modes including but not limited to: MS, MSMS, and SONAR. Making this an ideal platform for MS imaging applications, allowing each laboratory to tailor their imaging experiments to their specific needs.

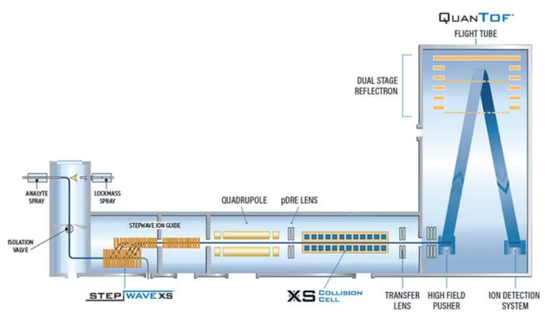

METHODS

A murine brain was sectioned at 18 µm onto glass microscope slides.

These sections were analysed with no further treatment on a Xevo G3 QTof mass spectrometer coupled to a DESI XS source with high-performance sprayer and heated transfer line.

Acquisition was performed in MS mode with mass ranges of 50-1200 Da.

Acquisition settings were as follows:

DESI source setup:

0.6 kV capillary voltage,

15 psi gas flow,

98% MeOH 2% Water solvent at 2 µL per minute.

The heated transfer line was set to 450 ºC.

Images were acquired with a pixel size of 50 µm and a step rate of 100, 250, 500 and 1000 µm/s giving equivalent scan speeds of: 2, 5, 10 and 20 scans per second for the acquisitions.

The resulting MS data were manually assessed using MassLynxTM software prior to being processed in High-Definition™ Imaging (HDI™) software for image visualization.

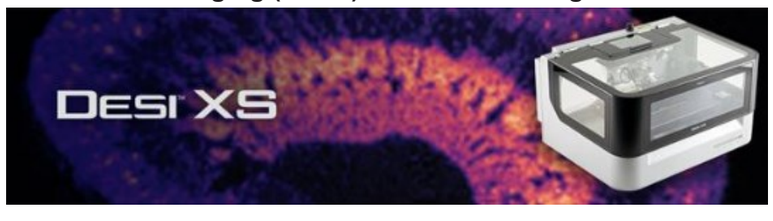

RESULTS & DISCUSSION

For each data set acquired with differing acquisition speeds distinct structures within the tissues were identified by segmentation mapping using the MSI segmentation MicroApp. This utilizes UMAP (Uniform Manifold Approximation and Projection) and HBDSCAN (Hierarchical Density-Based Spatial Clustering of Applications with Noise) for rapid spectral segmentation (*Figure2)*.

The segmentation analysis results were used to indicate boundaries of different structures within the tissues and can be seen to match closely between the differing acquisition speeds.

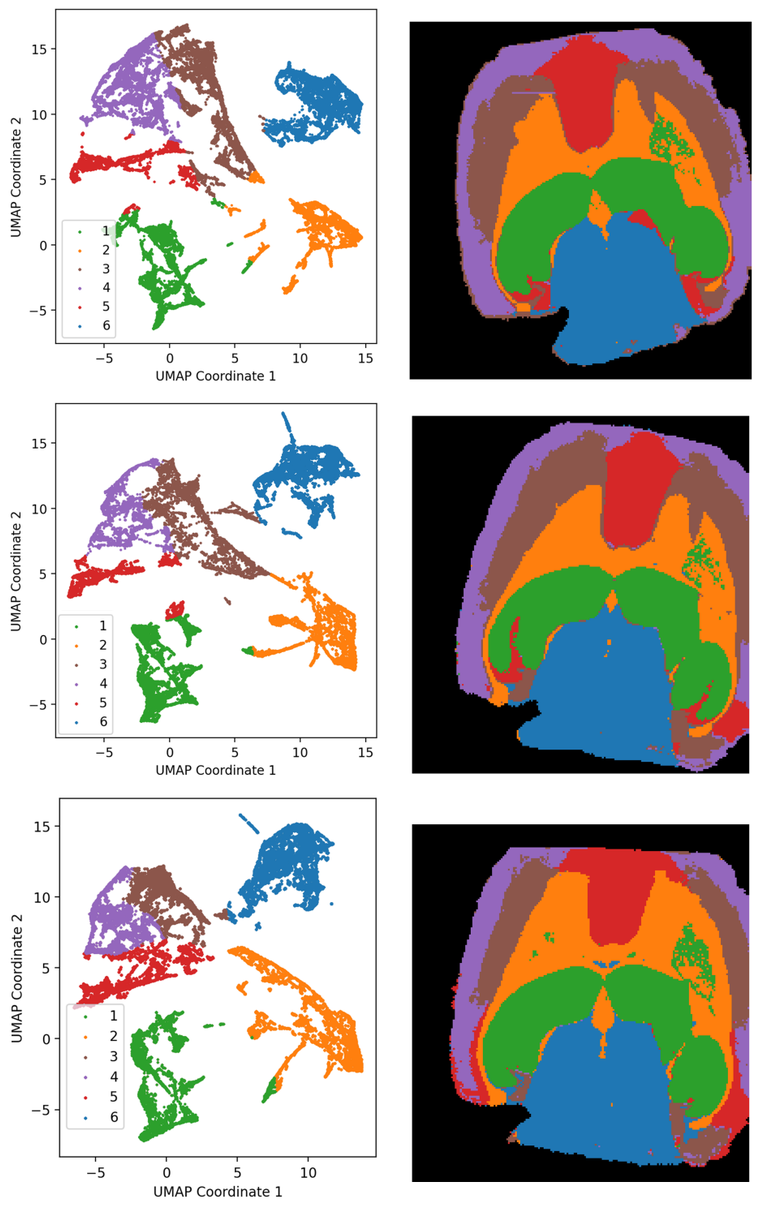

Figure 2: results of segmentation analysis for 5 scans/second (top) 10 scans/second (middle) and 20 scans/second (bottom). Minimum cluster size was 5% with 2 components and cosine as the Umap metric.

Utilizing the information provided by the segmentation tool four regions of interest (ROIs) were exported from each tissue structure for each of the acquisition speed datasets. *Figure 3.*

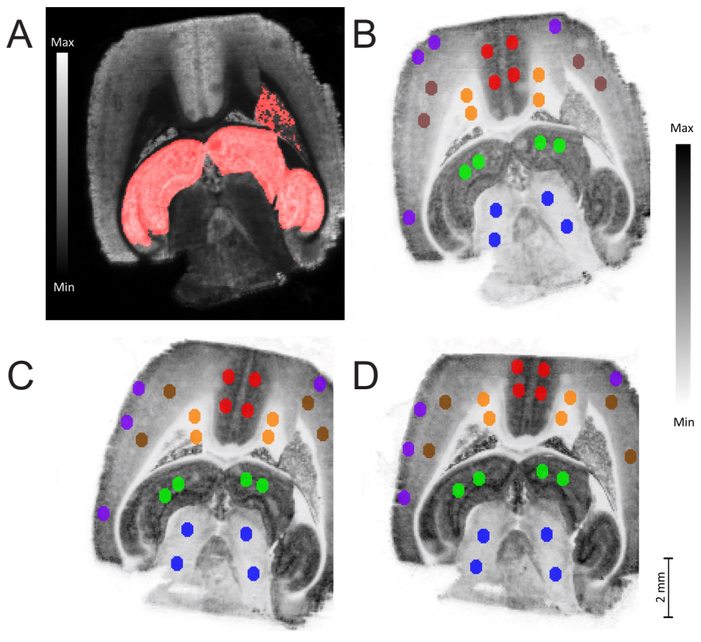

Figure 3: A) Example of segment mask imported in to HDI. B-D regions of interest exported from each acquisition speed (5-20 sps) selected using segment masks guides.

TIC normalization was utilized to compensate for signal reduction resulting from the increased acquisition speed, and the spectra for sub regions within the structures for each tissue were extracted.

Spectra from matching regions of interest showed a high degree of correlation between the different acquisition speeds. The resulting peak profiles were plotted against each other and assessed for similarity, by examining the slope and R^2 value of the plots.

Firstly the normal biological variation within the tissue sections was compared. Followed by scan speed variation.

Cluster #	5 sps	10 sps	20 sps
1	0.995 +/- 0.003	0.996 +/- 0.002	0.996 +/- 0.002
2	0.986 +/- 0.012	0.974 +/- 0.023	0.971 +/- 0.022
3	0.997 +/- 0.002	0.998 +/- 0.001	0.998 +/- 0.001
4	0.996 +/- 0.002	0.989 +/- 0.009	0.994 +/- 0.003
5	0.998 +/- 0.001	0.998 +/- 0.001	0.999 +/- 0.001
6	0.993 +/- 0.005	0.993 +/- 0.005	0.989 +/- 0.010

Table 1: demonstrates that biological variation between the tissue sections is small with a maximum R^2 value observed of > 0.97.

Cluster #	5 sps vs 10 sps	5 sps vs 20 sps	10 sps vs 20 sps
1	0.989 +/- 0.004	0.989 +/- 0.005	0.995 +/- 0.001
2	0.973 +/- 0.017	0.949 +/- 0.016	0.968 +/- 0.022
3	0.993 +/- 0.001	0.993 +/- 0.001	0.994 +/- 0.003
4	0.993 +/- 0.003	0.993 +/- 0.003	0.992 +/- 0.006
5	0.995 +/- 0.002	0.996 +/- 0.002	0.996 +/- 0.002
6	0.988 +/- 0.003	0.967 +/- 0.007	0.985 +/- 0.007

Table 2: shows good correlation between the differing speed with all the R^2 values obtained being > 0.949, including biological variance (Table 1).

When the ROIs (Figure 3) are imported into an unsupervised PCA each tissue region clearly clusters with little PCA separation observed due to scan speed.

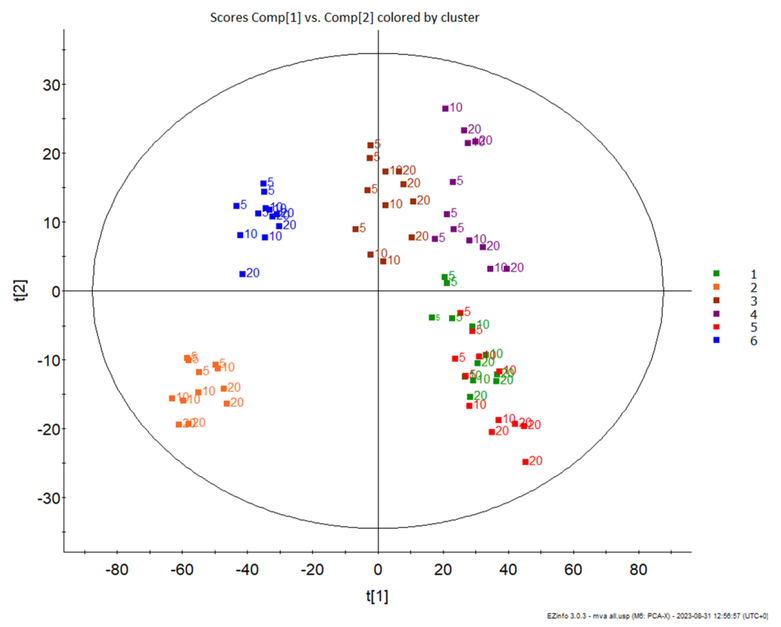

Figure 4: the unsupervised PCA plot generated when all ROIs from all three scan speeds are imported into a statistical software package.

Processing the consecutive murine brain sections, we were able to successfully identify key lipid markers of the prominent tissue regions in all acquired images (*Figure 1)*. We demonstrate that with increased acquisition speed there was no effect on the mass resolution (*Figure 5)* or mass accuracy of the resulting data *(Table 3).*

Theoretical mass (m/z)	Putative ID	Measured m/z and error (ppm)		
		5 sps	10 sps	20 sps
834.5290	PS(40:6)	834.5288 (-0.29)	834.5292 (+0.19)	834.5291 (+0.07)
810.5291	PS(38:4)	810.5266 (-3.01)	810.5276 (-1.78)	810.5281 (-1.16)
750.5443	PE(38:4)	750.5427 (-2.13)	750.5431 (-1.60)	750.5430 (-1.73)

Table 3: Mass accuracy for three lipids over the various scan speeds.

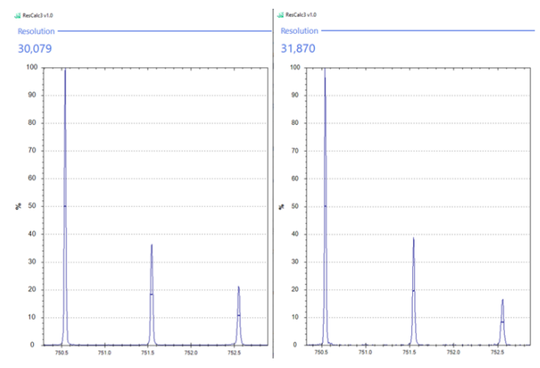

Figure 5: Mass resolution for a lipid with 5 sps and 20 sps scan speeds.

CONCLUSION

We have shown that increasing acquisition speed and reducing acquisition time does not appear to negatively impact data or image quality.

Due to improved instrument sensitivity, imaging speed can be increased whilst retaining excellent data quality for routine MS imaging applications.

We have demonstrated that despite a small reduction in signal with increased acquisition speed, the resulting spectral profiles are still highly correlated.

In addition, with increased acquisition speed there was no effect on the mass resolution or mass accuracy of the resulting data.

TO DOWNLOAD A COPY OF THIS POSTER, VISIT WWW.WATERS.COM/POSTERS